

hexan-2-*o*-l acetates, while X-1, X-2, and X-3 are (1 α ,2 α ,4 β)-4-alkylcyclohexan-2-*o*-l acetates. According to the IUPAC rules of organic nomenclature, these compounds are respectively *c*-4-alkyl-*t*-2-[2-²H₁]-*r*-1-cyclohexyl acetates and *t*-4-alkyl-*c*-2-[2-²H₁]-*r*-1-cyclohexyl acetates. The authors thank K. L. Loening, Nomenclature Director, Chemical Abstracts Service, for his assistance.

- (27) L. F. Fieser and M. Fieser, "Reagents for Organic Synthesis", Wiley, New York, 1967, pp 136-139.
 (28) V. J. Shiner, Jr., and J. S. Humphrey, *J. Am. Chem. Soc.*, **86**, 945-946

(1964).

- (29) B. Rickborn and J. Quartucci, *J. Org. Chem.*, **29**, 3185-3188 (1964).
 (30) G. Stork and W. N. White, *J. Am. Chem. Soc.*, **78**, 4604-4619 (1956).
 (31) Obtained from Pfaltz and Bauer, Inc.
 (32) E. L. Eliel and T. J. Brett, *J. Am. Chem. Soc.*, **87**, 5039-5043 (1965).
 (33) C. Djerassi, R. R. Engle, and A. Bowers, *J. Org. Chem.*, **21**, 1547-1549 (1956).
 (34) W. Hüchel and R. Bross, *Justus Liebigs Ann. Chem.*, **664**, 1-18 (1963).
 (35) E. E. Royals and A. N. Neal, *J. Org. Chem.*, **21**, 1448-1457 (1956).

Hydrogen Bonding of Water to Onium Ions. Hydration of Substituted Pyridinium Ions and Related Systems

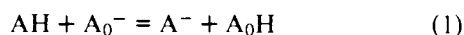
W. R. Davidson, J. Sunner, and P. Kebarle*

Contribution from the Department of Chemistry, University of Alberta, Edmonton, Canada T6G 2G2. Received August 3, 1978

Abstract: The hydration energies of substituted pyridinium ions were measured in the gas phase by determining the equilibrium constants for the gas-phase equilibria $XpyH^+(OH_2)_{n-1} + OH_2 = XpyH^+(OH_2)_n$. It was found that the hydrogen-bonding energies $XpyH^+ \cdots (OH_2)_n$ decrease with increasing basicity of the substituted pyridines Xpy. This decrease of solvation energy of the ions is largely responsible for the attenuation of the substituent effect on the pyridine basicities in aqueous solution. The gas-phase hydration energies show that a rather large number of water molecules must be present in the gas-phase hydration of the pyridinium ions before the relative solvation effects in aqueous solution are approached. A similar result is found for the substituted phenols. A general relationship between the acidity of oxygen and nitrogen onium acids BH^+ and the hydrogen bond in $BH^+ \cdots OH_2$ is explored. The hydrogen-bond energy is found to increase with the acidity of BH^+ . Largest hydrogen-bonding stabilization in $B_1HB_2^+$ is obtained when the basicities of B_1 and B_2 are equal. A qualitative molecular orbital model can explain these results.

Introduction

Comparison of the substituent effects on the acidities of phenols and benzoic acids in the gas phase and in solution can be made by plotting the differences of the free energies of ionization in the gas phase $\delta\Delta G_i(\text{gas})$ vs. the corresponding quantities in aqueous solution. $\delta\Delta G_i$ is defined as the free-energy change for the proton-transfer reaction



from AH, the substituted acid, to A_0^- , the unsubstituted conjugate base. The $\delta\Delta G_i(\text{gas})$ values are obtained from proton-transfer equilibria measured in the gas phase^{1,2} while $\delta\Delta G_i(\text{aqua})$ can be calculated from the pK_a values of the two acids in aqueous solution. Similar comparisons of the substituent effects in the gas phase and in solution can be made also for bases B and B_0 like substituted pyridines and pyridine.³ It is found that the plots of $\delta\Delta G_i(\text{gas})$ vs. $\delta\Delta G_i(\text{aqua})$ lead to fairly good linear relationships. However, the slopes of the straight lines are considerably larger than unity. For benzoic acids¹ the slope is 10, for phenols¹ 7, and for substituted pyridines³ about 3. This large attenuation of the substituent effect in solution must result from an effect of the substituent on solvation which partially cancels the effect of the substituent on the isolated molecule. It has been long recognized⁴ that the major factor involved in the attenuation must be the substituent effect on the solvation of the ions. For example, an electron-withdrawing substituent like CN, which increases the intrinsic acidity of phenol, is expected to unfavorably affect the solvation of the cyanophenoxide ion and thus reduce the acidity increase of cyanophenol in aqueous solution. Since this cancellation effect may be as large as 90% (benzoic acids), a linear relationship between gas phase and solution requires a fairly accurate proportionality between the substituent effect in the gas phase and the opposing ion solvation effect.

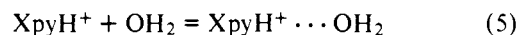
Some time ago, we reported^{5,6} a relationship between the basicity of A^- and the hydrogen bond in the monohydrate $A^- \cdots HOH$ which showed that the strength of the hydrogen bond increases with the (gas phase) basicity of A^- . Similarly it was found^{7,8} that the hydrogen bond in $BH^+ \cdots OH_2$ increases with the gas-phase acidity of BH^+ . These results were obtained by measurements of the gas-phase equilibria



As pointed out earlier,¹ the above relationships between the hydrogen bonding to a water molecule and the basicity of A^- or the acidity of BH^+ provide the answer, on a one molecule solvation basis for the attenuation mechanism in solution. Thus a substituent that increases the acidity of AH decreases the basicity of A^- and therefore decreases the hydrogen bonding in $A^- \cdots HOH$. The present work presents some new measurements of the hydration of substituted pyridinium ions in the gas phase and explores further the relationship between the acidity of BH^+ and the hydrogen bond in $BH^+ \cdots (OH_2)_n$. Some results relating to the analogous attenuation mechanism occurring in the phenols and hydrated phenoxide ions $A^- \cdots (HOH)_n$ are also included.

Results and Discussion

A. Hydrogen Bonding in $BH^+ \cdots OH_2$ and Related Systems. The equilibrium constants K_5 of the hydration equilibria



involving the substituted pyridinium ions $XpyH^+$ are shown in the van't Hoff plots in Figure 1. The ΔH_5° and ΔS_5° values obtained from these plots are given in Table I. As will be noticed from Table I, the entropy changes ΔS_5° are very similar and the small changes that are observed do not seem to fit a rational pattern. We assume that the observed ΔS differences

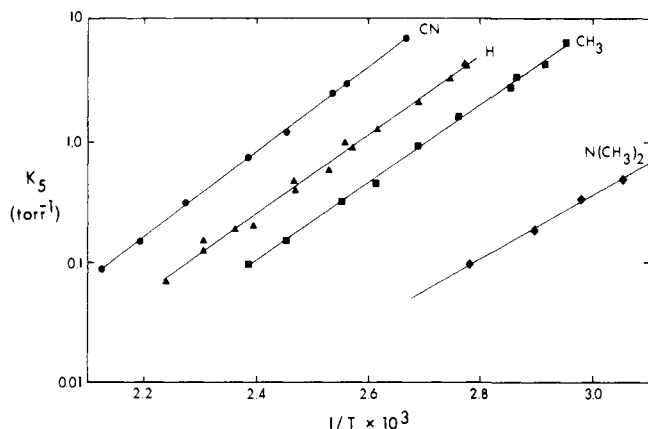


Figure 1. van't Hoff plots of equilibrium constants K_5 for reaction 5: $XpyH^+ + OH_2 = XpyH^+ \cdots OH_2$, where $XpyH^+$ are para-substituted pyridinium ions. Substituents X given over respective van't Hoff line.

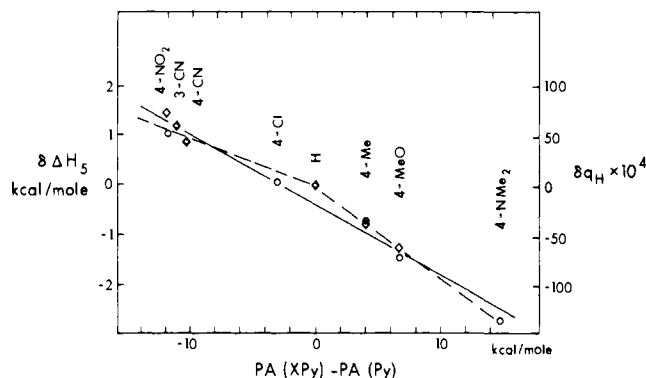


Figure 2. Plot showing that the strength of the hydrogen bond in $XpyH^+ \cdots OH_2$ increases with the gas-phase acidity of $XpyH^+$. $\delta\Delta H_5$ is the enthalpy change for the gas-phase reaction: $XpyH^+ \cdots OH_2 + pyH^+ = XpyH^+ + pyH^+ \cdots OH_2$. The difference between the proton affinities of pyridine and substituted pyridine $PA(py) - PA(Xpy)$ measures the difference between the acidities of $XpyH^+$ and pyH^+ . The proton affinities for the pyridines are taken from Arnett.³ δq_H shown on the vertical scale on the right gives the net atomic charge difference on the acidic H atom of the pyridinium ion. A δq_H of 0.01 units means that the acidic H on the substituted pyridinium has a positive charge that is 0.01 units higher than the charge on the unsubstituted pyridinium. These data are from Mezey et al.¹⁴ and are based on STO-3G calculations. The data show that both the relative proton affinities and the hydrogen-bonding energies are linearly related to the relative charge δq_H : O, $\delta\Delta H_5$ vs. δPA ; \diamond , δq_H vs. δPA .

are due to error in the van't Hoff plots, which do not extend over a wide enough temperature interval to provide ΔS° values which are accurate to more than ± 1 cal/deg. Since we are more interested in comparing the relative binding energies, a second set of "corrected" ΔH_5 values is given in column 5 of the table. These were obtained from $\Delta H_5(pyH^+) = -15$ kcal/mol and the measured $\Delta G_5^\circ(XpyH^+)$ values at 400 K and the assumption that the ΔS_5° values are the same (-25.6 cal/deg) for all substituents. This procedure allowed also the incorporation of equilibrium data for reaction 5 with additional substituents, which were obtained at a single temperature (400 K). Thus the relative enthalpies $\delta\Delta H_5$ given in the last column of the table are actually the $\delta\Delta G_5^\circ$ at 400 K.

A plot of the relative hydrogen bond energies, $\delta\Delta H_5$, vs. the proton affinities of the pyridines is shown in Figure 2. These results show that an increase of the acidity of the pyridinium ion leads to an increase in the hydrogen-bond energy in $XpyH^+ \cdots OH_2$. The relationship is approximately linear. It may be noted that the data are fitted better by two lines, one connecting the electron-donating substituents (Me_2N , MeO , and Me) and the other the electron-withdrawing substituents (Cl , NO_2 , and CN). Considering that the data are sparse and that

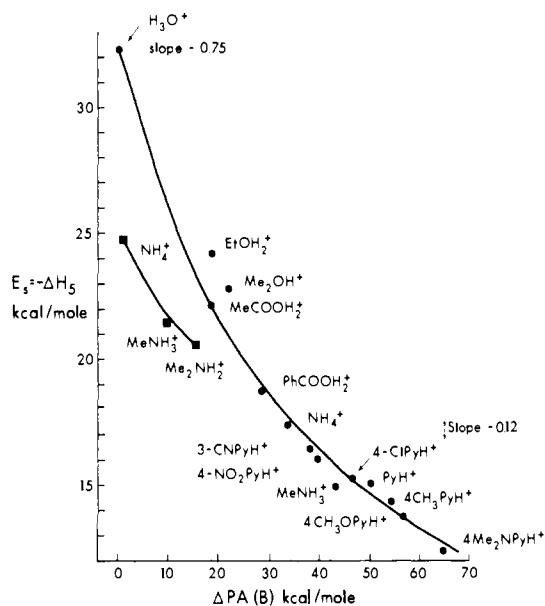


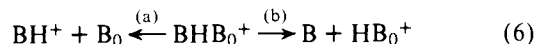
Figure 3. Relationship between the hydrogen bond energies in $BH^+ \cdots B_0$ and the proton affinity difference $PA(B) - PA(B_0)$: \bullet , $B_0 = H_2O$; \blacksquare , $B_0 = NH_3$. ΔH_5 is equal to enthalpy change for gas-phase reaction: $BH^+ \cdots B_0 = BH^+ + B_0$. Data for pyridine hydrates from this work; other data from ref 2. $PA(H_2O) = 168$ kcal/mol, $PA(NH_3) = 202$ kcal/mol.² Results show that the hydrogen bond in $BH^+ \cdots B_0$ is maximum for $\Delta PA(B) = 0$ and decreases as the acidity of BH^+ is decreased.

there is some experimental error involved, we believe that the two different slopes for the two different types of substituents indicated by the data are not a real effect but are due to an accidental scatter of the data points.

The relationship between the acidity of BH^+ and the strength of the hydrogen bond in $BH^+ \cdots OH_2$ is extended over a much wider range of onium compounds in the data shown in Figure 3. This figure includes the pyridinium acids and other onium acids like NH_4^+ , $MeOH_2^+$, and H_3O^+ . The additional data used in Figure 3 were taken from ref 2. The H-bond energies observed with the wide range of BH^+ acidities do not obey a straight-line relationship;⁹ however, a fair fit of all the data can be obtained by a single curve. The slope for the weak onium acids like the pyridinium ions is -0.12 while the largest (absolute) slope (-0.75) is observed for the strongest acid, H_3O^+ . The (absolute) slope may be related to the degree of proton transfer from BH^+ to OH_2 . With the weak pyridinium acids there is little proton transfer to OH_2 and a small slope while for the stronger acid H_3O^+ there is considerable proton transfer and a large slope.

Also shown in Figure 3 is a second series in which the constant reference base is ammonia and the acids are the methyl- and dimethylammonium ions. These data were taken from previous determinations from this laboratory.² This set is much more limited but the results are similar to those observed for the H_2O series.

Calling the constant base B_0 , and considering the equation



one finds that the H-bond energies represented in Figure 3 correspond to the dissociation via path (a). The data in Figure 3 are restricted to cases where the acidity of BH^+ is lower (or equal) to that of B_0H^+ , i.e., $PA(B) - PA(B_0) > 0$. Of course, the curves could be extended to the region where $PA(B) - PA(B_0) < 0$, i.e., into the negative region of the x axis of Figure 3. One expects the curves to extrapolate continuously into this region. This means that the H-bond energies $BH^+ \cdots B_0$ will increase beyond $B_0H^+ \cdots B_0$ and the slope will also increase up

Table I. Thermodynamic Data^a Obtained from Equilibria Measurements for Reaction 5
$$\text{X-C}_5\text{H}_4\text{N-H}^+ + \text{OH}_2 = \text{X-C}_5\text{H}_4\text{N-H}^+ \cdots \text{OH}_2$$

X	$-\Delta H_5^b$	$-\Delta S_5^b$	$-\Delta G_5^b(400)^c$	$-\Delta H_5^b(\text{cor})^d$	$\delta\Delta H_5 = \delta\Delta G_5^e$
4-CN	16	25.7	5.7	15.9	-0.9
H	15	25.5	4.8	15.0	0
4-CH ₃	14.7	26.6	2.1	14.3	0.7
4-N(CH ₃) ₂	12.0	24.8	6.0	12.3	2.7
3-CN			6.0		-1.2
4-NO ₂			5.9		-1.1
4-Cl			4.9		-0.1
4-OCH ₃			3.4		1.4

^a All energies in kcal/mol, entropies in cal deg⁻¹ mol⁻¹, standard state 1 atm. ^b From van't Hoff plots (Figure 1). ^c Free-energy change measured at 400 K. ^d Enthalpy change calculated from $\Delta G_5(400)$ and $-\Delta S_5 = 25.6$ cal/deg assumed constant for all substituents. ^e Energy change for reaction $\text{XpyH}^+ + \text{pyH}^+\text{-OH}_2 = \text{XpyH}^+ \cdots \text{OH}_2 + \text{pyH}^+$.

Table II. Thermodynamic Data^a for Stepwise Hydration of Pyridine and 4-Cyanopyridine: $\text{XpyH}^+(\text{OH}_2)_{n-1} + \text{OH}_2 = \text{XpyH}^+(\text{OH}_2)_n$

X	$n-1, n$	$-\Delta H^\circ$	$-\Delta S^\circ$	$-\Delta G^\circ$ ^c	temp, °C	$\delta\Delta H^\circ$ ^b	$\delta\Delta G^\circ$ ^{b,c} ($\approx \delta\Delta H^\circ$)
H	0, 1	15.0 ± 0.3	25.5 ± 0.9	4.76	127		
	1, 2	9.6 ± 0.3	19.6 ± 0.9	4.25	0		
	2, 3	8.3 ± 0.5	19.6 ± 2.0	3.37	-23		
4-CN	0, 1	16.0 ± 0.3	25.7 ± 0.9	5.66	127	-1.0	-0.9
	1, 2	10.4 ± 0.3	20.2 ± 1.0	4.87	0	-0.8	-0.6
	2, 3	8.9 ± 0.2	20.2 ± 0.9	3.89	-23	-0.6	-0.5
	3, 4	8.2 ± 0.8	19.7 ± 3.3				

^a Energies in kcal/mol, entropies in cal deg⁻¹ mol⁻¹. Standard state 1 atm. ^b For reaction $\text{pyH}^+ \cdots (\text{OH}_2)_n + \text{CNpyH}^+ \cdots (\text{OH}_2)_{n-1} = \text{pyH}^+ \cdots (\text{OH}_2)_{n-1} + \text{CNpyH}^+ \cdots (\text{OH}_2)_n$. ^c For temperature given in sixth column of table. This temperature corresponds to middle of temperature range of van't Hoff plot.

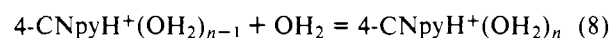
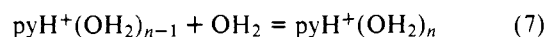
to a limiting slope of approximately unity for $\text{PA}(\text{B}_0) \gg \text{PA}(\text{B})$. One experimental point of this kind is available for the $\text{B}_0 = \text{NH}_3$ curve. This is the H-bond energy $\text{NH}_3\text{-H}_3\text{O}^+$, which is 50 kcal/mol for $\text{PA}(\text{B}) - \text{PA}(\text{B}_0) = -33$ kcal/mol (the $\text{NH}_3\text{-H}_3\text{O}^+$ dissociation energy is obtained by adding $\text{PA}(\text{NH}_3) - \text{PA}(\text{H}_2\text{O}) = 33$ kcal/mol to the $\text{NH}_4^+\text{-H}_2\text{O}$ dissociation energy of 17 kcal/mol (see eq 6)). The cases in the negative region of the x axis considered above correspond to dissociation via the more endothermic path (b). Although it is useful to know how the curves in Figure 3 will extrapolate into the negative $\text{PA}(\text{B}) - \text{PA}(\text{B}_0)$ region, the stabilization due to H bonding in BHB_0^+ is more meaningfully defined if one considers only the less endothermic path (a). With this definition maximum stabilization occurs for B_0HB_0^+ .

The results in Figure 3 are in line with predictions based on molecular orbital considerations. We will consider only bases B and B_0 which have similar lone-pair orbitals, as is the case for the present nitrogen and oxygen compounds. The hydrogen bonding in $\text{H}_3\text{NHNH}_3^+$ has been described by Peyerimhoff¹¹ as resulting mostly from the $5a_1$ MO. This orbital represents essentially the in-phase addition of the two nitrogen lone pairs. The $6a_1$ MO, which represents essentially the out of phase combination of the lone pairs, is, in the absence of the 1s AO of the bridging proton, very nearly of the same energy as the $5a_1$. The presence of the 1s AO brings about a large lowering of the $5a_1$ orbital, which interacts strongly with the 1s, while the $6a_1$ MO is affected little. Thus the $5a_1$ MO is essentially the only orbital which represents the hydrogen bridge.¹¹ If we consider now the case where two different bases are involved, i.e., BHB_0^+ , the MO representing the in-phase combination of the lone-pair orbitals plus the 1s orbital of the proton will be of low energy and lead to a strong H bond when the overlap of the lone pairs is large and when their energy is close to equal. One may take the ionization potentials of the lone pairs in B and B_0 as an approximate measure of the energies of the corresponding lone-pair orbitals. Since the ionization potentials of the lone pairs are approximately (inversely) proportional

to the proton affinities, the energy lowering for the in-phase combination of the lone-pair orbitals will be maximum for $I_p(\text{B}) = I_p(\text{B}_0)$, i.e., $\text{PA}(\text{B}) \approx \text{PA}(\text{B}_0)$, and decrease as the difference between the ionization potentials and the difference between the proton affinities increases. This is in exact accord with the results shown in Figure 3.

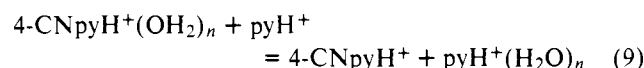
A schematic representation of the dependence of the stabilization due to H bonding, the degree of proton transfer, and the difference of the proton affinities is given in Figure 4.

B. Gas-Phase Hydration by More Than One Water Molecule and Hydration Energies in the Liquid Solvent. The preceding section dealt with the hydration energies of the ions by one water molecule. We will now consider ion hydration by more than one molecule. van't Hoff plots for the equilibria



measured in the present work are shown in Figure 5. These plots lead to the enthalpy and entropy changes which are shown in Table II. Unfortunately equilibria only up to four water molecules could be measured, since, at temperatures low enough for further hydration, condensation of water occurred on the wall of the ion source-reaction chamber. This means that the vapor pressure of the hydrates with $n > 4$ is larger than that of condensed water at the same temperature. The results in Table II show, as expected, that the hydrations of the stronger pyridinium acid are more exothermic for all n , and that the difference of the hydration energies of the two pyridinium ions decreases gradually with n . Since $\Delta S^\circ_{n-1,n}$ is approximately the same for cyanopyridinium and pyridinium, one finds $\delta\Delta H_{n-1,n} \approx \delta\Delta G_{n-1,n}$.

From the data in Table II one can evaluate the enthalpy (\approx free energy) change for the water transfer reaction



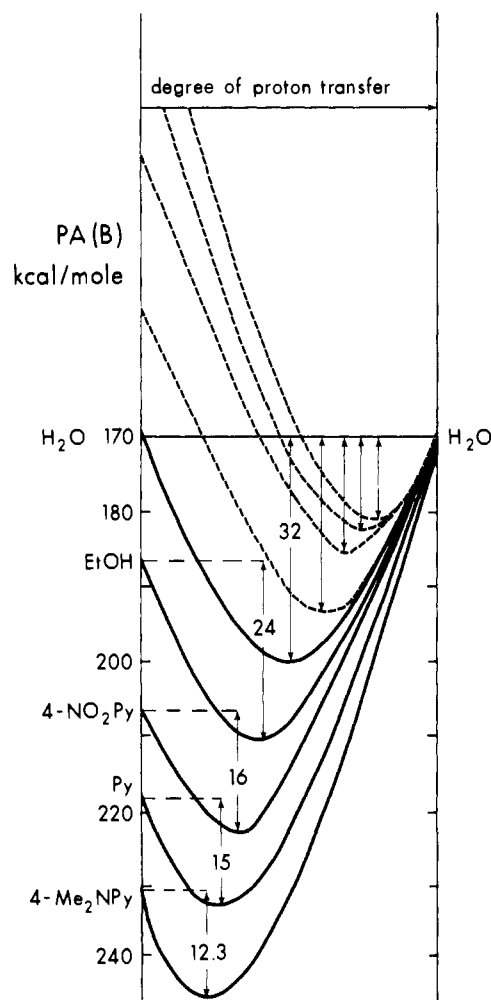


Figure 4. Plot of stabilization energies E_s due to H bonding corresponding to ΔH for dissociation $\text{BH}^+\text{OH}_2 = \text{BH}^+ + \text{OH}_2$ (solid curves) and $\text{BH}^+\text{OH}_2 = \text{B} + \text{OH}_3^+$ (dashed curves). The E_s of the solid curves are actual experimental data (see Figure 3). The E_s of the dashed curves are hypothetical, since no data for oxygen bases with lower PA than water are available. The degree of proton transfer from BH^+ to OH_2 (i.e., horizontal coordinate) is arbitrarily chosen. Results show that maximum E_s , i.e., maximum hydrogen bonding, is obtained when $\text{PA}(\text{B}) = \text{PA}(\text{H}_2\text{O})$. For correlation between E_s , $\text{PA}(\text{B})$, and $\text{PA}(\text{H}_2\text{O})$ by a qualitative molecular orbital argument see text.

Using the notation $\Delta H_0 = \delta\Delta H_{0,n}^{\text{H}_2\text{O}}(\text{CNpyH}^+)$, we expect that for large n this quantity should become equal to the difference of the hydration energies of the corresponding two ions in liquid water shown in the equation

$$\delta\Delta H_{0,n}^{\text{H}_2\text{O}}(\text{CNpyH}^+) = \Delta H_{0,n}^{\text{H}_2\text{O}}(\text{CNpyH}^+) - \Delta H_{0,n}^{\text{H}_2\text{O}}(\text{pyH}^+) \quad (10)$$

The change of $\delta\Delta H_{0,n}$ with n is shown in Figure 6. Arnett and Taft³ have recently examined the gas and aqueous basicities of substituted pyridines. By means of Born-type cycles involving the gas phase and the aqueous proton transfer reactions as well as associated thermochemical data, these authors were able to obtain the relative hydration energies of the substituted pyridinium ions. The $\delta\Delta H_{0,n}^{\text{H}_2\text{O}}(\text{4-CN-pyH}^+)$ obtained in this manner by Arnett and Taft^{3,12} is shown in Figure 6. Evidently the n molecule transfer enthalpy $\delta H_{0,n}$ at $n = 3$, the highest n for which results are available, is still a long way off from the $\delta\Delta H_{0,n}^{\text{H}_2\text{O}}$.

Included in Figure 6 is a point corresponding to ΔE obtained by Hehre³ from the LCAO-MO (STO-3G) calculated energies of the reactants in reaction 9 with $n = 1$. This ΔE should be approximately equal to $\delta\Delta H_{0,1}$. The calculated results $-\Delta E$

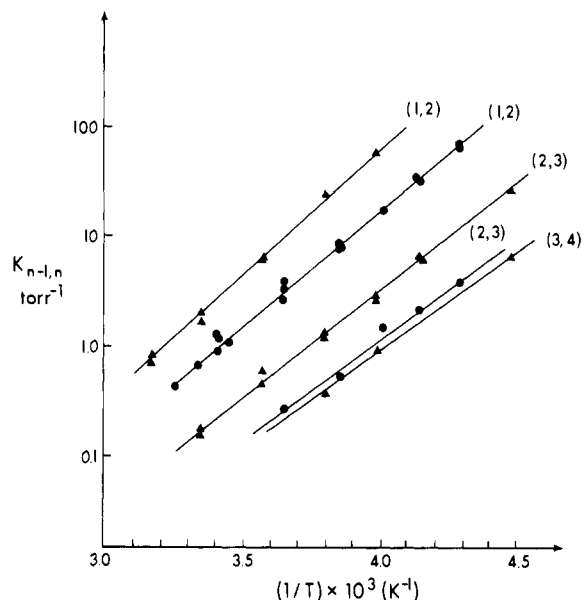
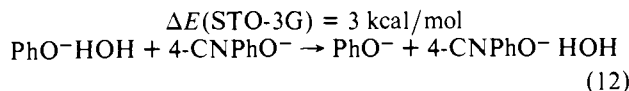
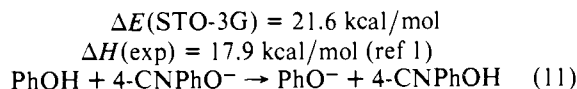


Figure 5. van't Hoff plot of reactions: $\text{pyH}^+(\text{H}_2\text{O})_{n-1} + \text{H}_2\text{O} = \text{pyH}^+(\text{H}_2\text{O})_n$ ●; $\text{4-CN-pyH}^+(\text{H}_2\text{O})_{n-1} + \text{H}_2\text{O} = \text{4-CN-pyH}^+(\text{H}_2\text{O})_n$ ▲.

$= 1.9$ kcal/mol is about twice as large as the experimentally measured $-\delta\Delta H_{0,1} = 1$ kcal/mol. However, when energy changes as small as 1 kcal/mol are involved one cannot expect anything better from the calculation.

As mentioned earlier, the attenuation of the aqueous acidities of the phenols has the same hydrogen-bonding origin as the attenuation of the pyridine basicities.¹ We hope to be able to provide in the near future experimental measurements of the gas-phase hydrations of the phenoxide negative ions. For the present we can offer some results from STO-3G calculations which are of some interest. The STO-3G calculated (see the section Experimental and Calculations) hydration difference of phenoxide and 4-cyanophenoxide represented in reaction 12 was found to be $\Delta E_{12} = 3$ kcal/mol.

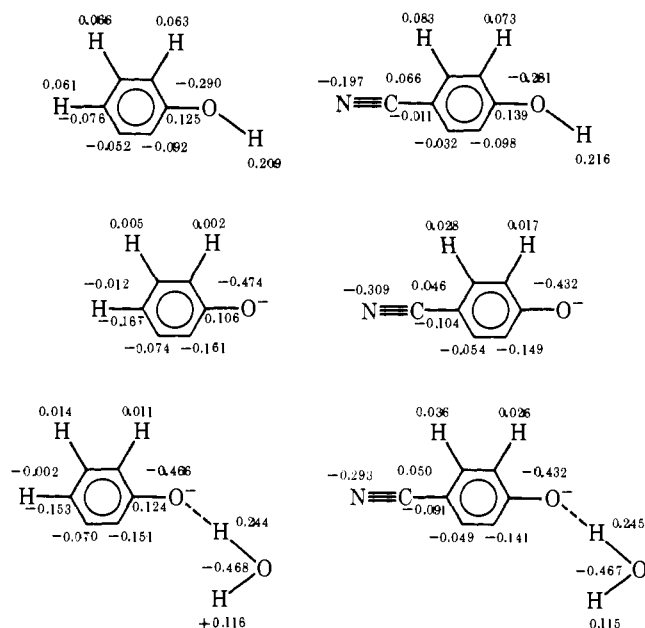


Reaction 11 gives the molecular acidity difference between phenol and 4-cyanophenol. For this reaction experimental measurements ΔH_{exp} are also available.¹ From (11) and (12) it is evident that the hydrogen-bonding trend follows the expected change with change of basicity of A^- , i.e., the anion of the stronger acid, cyanophenol, hydrogen bonds more weakly to water than the unsubstituted phenoxide. The $-\Delta E_{12}/\Delta E_{11} = -0.14$ represents the slope of a relationship analogous to that shown in Figure 2. This slope is quite similar to that observed for the pyridinium ions, which was -0.12 . The present situation is similar to that for the pyridines since only minimal proton transfer occurs from the weak acid HOH to the weak phenoxide bases PhO^- . The difference between the hydration enthalpies of PhO^- and CNPhO^- , $\delta\Delta H_{0,n}^{\text{H}_2\text{O}}(\text{A}^-)$, may be estimated from results of Arnett¹³ to be 80% of the gas phase acidity difference. This leads to $\delta\Delta H_{0,n}^{\text{H}_2\text{O}}(\text{A}^-) \approx 16$ kcal/mol (for CNPhO^-). The difference in hydrogen-bonding energies for one water molecule predicted by STO-3G (eq 12) was 3 kcal/mol. This means that the first hydration step pro-

vides only ~20% of the total solvation energy difference of ≈ 16 kcal/mol observed in liquid water. Therefore, as in the case of the pyridinium ions, we find that the cooperative effect of a rather large number of water molecules is required to achieve the total difference $\delta\Delta H_{\text{E}^{\ominus} \rightarrow \text{H}_2\text{O}}(\text{A}^-)$ in liquid water.

The observation that both for the substituted pyridines and phenols the addition of a few water molecules leads to an attenuation of the substituent effect which is much smaller than the attenuation observed in liquid water may be explained on basis of two effects. One of these is the increasing H-bonding effect as the cluster of water molecules H bonded to the functional group grows. For the pyridinium ions the basicity of the $(\text{HOH})_n$ grows with n , while for the phenoxide ions it is the acidity of the $(\text{HOH})_n$ that grows. This duality is expected for water since a cluster of H-bonded water molecules will interact favorably with both a partial proton and a partial O^- . The second factor involved in the need for large n should be connected with the field effect of the substituent dipole. In liquid water the field effect of the substituent dipole is attenuated by the high dielectric constant of the aqueous medium. In the gas-phase hydrates $\text{XpyH}^+(\text{OH}_2)_n$ and $\text{XPhO}^-(\text{HOH})_n$, for small n , the H-bonded water molecules cluster around the ionic functional group, and do not provide a water molecule network to the substituent. Therefore, little dielectric attenuation of the substituent dipole can occur. Probably a substantial fraction of the difference between $\delta\Delta H_{0,3}$ and $\delta\Delta H_{\text{h}}$ in Figure 6 is due to the absence of the dielectric attenuation in the gas-phase trihydrates.

The geometries and net atomic charges obtained by the STO-3G calculations for the phenoxide ions and the monohydrates are shown below. As expected, the net negative charge on the oxygen of the phenoxide is noticeably higher than that for the cyanophenoxide. The negative charge on the CN nitrogen (-0.309 electrons) of the phenoxide originates from



hydrates

$r \text{O} \cdots \text{H}$	1.587 Å	1.551 Å
C-O-H angle	118.6°	124.3°

the charge withdrawal from the oxygen and an additional much larger charge withdrawal from the aromatic ring. Reynolds, Mezey, Hehre, Topsom, and Taft¹⁴ have shown that δq_{H} , which represents the difference between the net atomic charge on the protic hydrogen on the substituted and unsubstituted pyridinium ions, is proportional to the relative acidity of the pyridinium ions. These results are displayed in Figure 2 of the present work. Because of the proportionality between

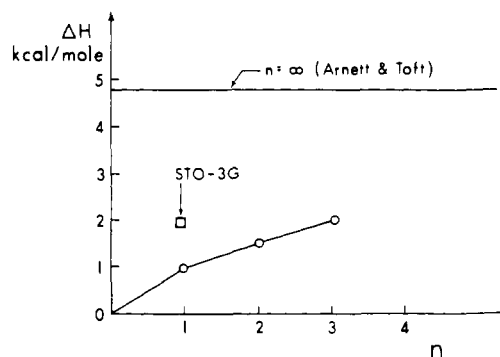


Figure 6. Enthalpy change for reaction $4\text{-CN-pyH}^+ \cdots (\text{OH}_2)_n + \text{pyH}^+ = 4\text{-CN-pyH}^+ + \text{pyH}^+ \cdots (\text{OH}_2)_n$ vs. n . Results for $n = \infty$ correspond to difference of hydration energies: $\Delta H_{\text{E}^{\ominus} \rightarrow \text{H}_2\text{O}}(4\text{-CN-pyH}^+) - \Delta H_{\text{E}^{\ominus} \rightarrow \text{H}_2\text{O}}(\text{pyH}^+)$ in liquid water obtained by Arnett and Taft³ from the gas-phase and aqueous basicities of the pyridines and Born-type cycles. Result from STO-3G calculation.³

the hydrogen bonding in $\text{XpyH}^+ \cdots \text{OH}_2$ and the acidities of XpyH^+ , it follows that the hydrogen bond energies also change linearly with δq_{H} of the pyridinium ions. For the phenoxide ions a similar relationship is expected. The negative charge on the oxygen should decrease linearly with decrease of the basicity of the phenoxides and the hydrogen bond strength in $\text{XPhO}^- \cdots \text{HOH}$.

Considering the hydrogen bond as a largely electrostatic interaction one may ask whether STO-3G predicted change of the charge on the functional group of the ion is sufficient to explain the change in the hydrogen-bonding energies. Unfortunately, this question cannot be answered unequivocally. Improved electrostatic calculations, which were found quite successful¹⁵ in predicting binding energies involving the spherical alkali or halide ions to a number of solvent molecules, cannot be directly applied to the nonspherical phenoxide ions. Calculations using the same equations¹⁵ but in which the ion-dipole attraction included only the partial negative charge on the phenoxide oxygen and the ion-water repulsion was expressed only by a phenoxide oxygen-water¹⁶ repulsive parameter were made for the present work. This approach has some approximate validity since the other partial charges on the phenoxide, being farther removed, should contribute not more than 20% to the binding energies. The calculations predict higher binding energies not for the linear $\text{O} \cdots \text{H} - \text{O}$ bonded monohydrate but for the bifurcated H bond in which the two hydrogens of the water interact symmetrically with the negative center. This is a common result for the electrostatic calculations.¹⁵ The binding energies obtained using the STO-3G partial charges of -0.474 and -0.432 for the oxygen in the phenoxide and cyanophenoxide are 6.7 and 6.9 kcal/mol. These energies when compared to available experimental values for related systems² appear far too small. Scaling¹⁷ the charges up to -0.78 and -0.71 (scaling factor 1.7) one obtains 13.2 and 11.6 kcal/mol as binding energies. These values are more reasonable. The difference of 1.6 kcal is still considerably smaller than the $\Delta E(\text{STO-3G}) = 3$ kcal/mol (see reaction 12), but the validity of this STO-3G result is also questionable. We may conclude tentatively that the STO-3G predicted differences of charge on the oxygen of the substituted phenoxides are lower than what might be required to explain the hydrogen-bonding differences from a purely electrostatic standpoint. The same is probably also true for the even smaller charge differences on the protic hydrogens of the pyridinium ions.

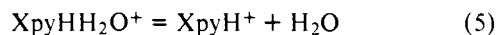
Experimental and Calculations

The experimental measurements were made with a pulsed electron beam high ion source pressure mass spectrometer which has been described previously.²

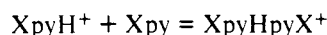
The measurements of the pyridinium hydration equilibria were made in ~4 Torr of methane containing water vapor in the 0.2–1 Torr range. The water used contained $\sim 1 \times 10^{-2}$ mol % pyridine such that a pressure of less than 10^{-4} Torr of pyridine resulted in the ion source. Under these conditions, protonation of water by the methane ions, CH_5^+ and C_2H_5^+ , is fast. Rapid clustering reactions lead to $\text{H}^+(\text{H}_2\text{O})_n$. Protonation and hydration of the pyridines occurs by the reaction



By suitable choice of temperature, the equilibria



can be made to occur appreciably faster than the dimerization reaction



This reaction is slow since the Xpy concentration is very low. The equilibrium constants K_5 were found to be constant in the range between 0.2 and 0.8 Torr water pressure.

The higher hydration equilibria (7) and (8) were measured similarly but at correspondingly lower temperatures. The water pressure range over which they could be observed was narrower than was the case for the monohydrates.

The STO-3G calculations of the phenols, phenoxides and monohydrates were made with the GAUSSIAN 70 program.¹⁸ In general the standard geometries outlined by Pople and Gordon¹⁹ were used except for the following: phenol, the carbon–oxygen bond distance and the COH angle were optimized; phenoxide ion, the carbon–oxygen bond was optimized; cyanophenol, carbon–oxygen distance and COH angle were optimized; cyanophenoxide, C–C_{arom}, C≡N, and C–O bonds were optimized, but optimum distances were essentially the same as in cyanophenol; hydrates, O...H–O distance and O...H–O angle was optimized.

Acknowledgment. The discussion of this work benefited from some useful suggestions by Professor R. W. Taft. The financial support of the Canadian National Research Council is gratefully acknowledged.

References and Notes

- (1) T. B. McMahon and P. Kebarle, *J. Am. Chem. Soc.*, **99**, 2222 (1977).
- (2) P. Kebarle, *Annu. Rev. Phys. Chem.*, **28**, 445 (1977).
- (3) E. M. Arnett, B. Chawla, L. Bell, M. Taagepera, W. J. Hehre, and R. W. Taft, *J. Am. Chem. Soc.*, **99**, 5729 (1977).
- (4) J. F. Coetzee and C. D. Ritchie, Eds., "Solute Solvent Interactions", Marcel Dekker, New York, 1969.
- (5) J. D. Payzant, R. Yamdagni, and P. Kebarle, *Can. J. Chem.*, **49**, 3308 (1971).
- (6) R. Yamdagni and P. Kebarle, *J. Am. Chem. Soc.*, **93**, 7139 (1971).
- (7) R. Yamdagni and P. Kebarle, *J. Am. Chem. Soc.*, **95**, 3504 (1973).
- (8) K. Hiraoka, E. P. Grimsrud, and P. Kebarle, *J. Am. Chem. Soc.*, **96**, 3359 (1974).
- (9) A straight-line relationship had been assumed in earlier work^{5,6} from results which used older and insufficient thermochemical data. More recent results¹⁰ for the hydrogen bond in $\text{AH} \cdots \text{Cl}^-$ vs. the gas-phase acidity of oxy acids AH showed similar curvature as seen in Figure 3. Carbon acids AH did not fit in the above plot but gave very much weaker bonded complexes.
- (10) P. Kebarle, W. R. Davidson, M. French, J. B. Cumming, and T. B. McMahon, *Discuss. Faraday Soc.*, **64**, 220 (1977).
- (11) P. Merlet, S. D. Peyerimhoff, and R. J. Buenker, *J. Am. Chem. Soc.*, **94**, 8301 (1972).
- (12) Arnett and Taft³ on the basis of extrathermodynamic considerations were able to separate the hydrogen-bonding part of the water solvation of the pyridinium ions from the other terms (cavity formation and structural changes in solvent). However, for cyanopyridine the $\delta\Delta H^\ddagger + \text{H}_2\text{O} = -4.8$ kcal/mol is almost identical with the $\delta\Delta H^\ddagger + \text{H}_2\text{O}$ due to H bonding only, which is -5 kcal/mol.
- (13) E. M. Arnett, L. E. Small, D. Oancea, and D. V. Johnston, *J. Am. Chem. Soc.*, **98**, 7346 (1976).
- (14) W. F. Reynolds, P. G. Mezey, W. J. Hehre, R. D. Topsom, and R. H. Taft, *J. Am. Chem. Soc.*, in press.
- (15) W. R. Davidson and P. Kebarle, *J. Am. Chem. Soc.*, **98**, 6133 (1976).
- (16) The general outline of the calculations is given in ref 15. While only the charge and repulsive parameter of the phenoxide oxygen were taken to represent the negative ion, the dispersion forces were calculated by considering the complete phenoxide ion.
- (17) A scaling by a factor of ~ 1.7 of STO-3G calculated net atomic charges in various molecules was required¹⁵ in order to obtain the experimental dipole moments.
- (18) W. J. Hehre, W. A. Lathan, R. Ditchfield, M. D. Newton, and J. A. Pople, GAUSSIAN 70, Quantum Chemistry Program Exchange, Indiana University, Bloomington, Ind.
- (19) J. A. Pople and M. Gordon, *J. Am. Chem. Soc.*, **89**, 4253 (1967).

Remote Secondary Deuterium Kinetic Isotope Effects as a Probe of Steric Strain in the Solvolysis of Tertiary Alkyl Carbinyl Systems¹

Robert C. Badger and James L. Fry*

Contribution from Bowman-Oddy Laboratories, Department of Chemistry, The University of Toledo, Toledo, Ohio 43606. Received September 20, 1978

Abstract: The kinetic isotope effects associated with the solvolysis of 9-*tert*-butyl-9-bicyclo[3.3.1]nonyl (**3**), 2-*tert*-butyl-2-adamantyl (**4**), and 2-*tert*-butyl-*endo*-camphenyl (**5**) *p*-nitrobenzoates, completely deuterated at the *tert*-butyl groups, were found in 95.6% aqueous ethanol at 25 °C to be ($k_{\text{H}}/k_{\text{D}}$) 1.030, 1.107, and 1.076, respectively. Compound **3** gave primarily unrearranged alcohol (7.7%) and the methyl-shifted alkene 9-(2'-propenyl)-9-methylbicyclo[3.3.1]nonane (88.4%) as solvolysis products. A preference for CH_3 migration over CD_3 migration by a factor of 1.35 was observed. Compound **4** similarly yielded unrearranged alcohol (6.9%) and the methyl-shifted alkene 2-(2'-propenyl)-2-methyladamantane (90.2%) and showed a preference for CH_3 over CD_3 migration in product formation by a factor of 1.25. The kinetic isotope effects are interpreted in terms of relief of constraints on vibrational freedom at the positions of isotopic substitution during the activation process. The kinetic isotope effects did not correlate well with the *t*-Bu/ CH_3 substituent effects.

The problem of understanding the origins of chemical reactivity is a vexing one. Steric effects, together with effects of electronic origin, are important in governing chemical reactivity. It is now a generally accepted principle that relief of

initial state steric strain can result in enhanced rates of solvolysis for sterically congested tetragonal molecules (**1**) which decompose in a unimolecular rate-controlling step to a trigonal, planar carbocation (**2**).² There is less agreement, however, on